8th International Work shop on Astronomy and Relativistic Astrophysics 2018 Peru

Investigation of the Ohmic decay and the soft X-ray emission of high- braking index pulsar PSR J1640-4631

Zhi-Fu Gao Shan Hao** Hui Wang***

** Xinjiang Astronomical Observatory, Chinese Academy of Sciences, Urumqi, Xinjiang, China. email: zhifugao@xao.ac.cn

* School of Physical Science and Technology, Southwest Jiaotong University, Chengdu, SichuanChina

Outline

- Background
- The Ohmic decay of dipole magnetic fields in PSR J1640-4631
- The coupled model of the ohmic decay and Hall drift
- Anisotropic heating for soft X-ray emission
- Summarry

Sec.1 Background

- A pulsar spins down with a power law

$$\dot{\Omega} = -k\Omega^n \qquad (1a)$$

- The braking index is defined as

$$n = \frac{\Omega\ddot{\Omega}}{\dot{\Omega}^2} = \frac{\nu\ddot{\nu}}{\dot{\nu}^2} = 2 - \frac{P^2\ddot{P}}{\dot{P}^2} \qquad (1b)$$

- There are 8 pulsars with measured braking index, 7 has $n < 3$ and one has $n > 3$, which deviate from expected value $n = 3$ by the magneto-dipole radiation model

Braking indexes of 8 magnetars with SNRs

Source	n	Timing reference
1E 1841	13 ± 4	Dib & Kaspi (2014)
SGR 0526	2.40 ± 0.04	Tiengo et al. (2009)
	$1.82 \pm 0.06^*$	Kulkarni et al. (2003)
SGR 1627	1.87 ± 0.18	Esposito et al. (2009a,b)
SGR 0501	6.3 ± 1.7	GöğüS et al. (2010)
PSR J1622	$>2.35 \pm 0.08$	Levin et al. 2010
	$>2.6 \pm 0.6^*$	Levin et al. 2010
1E 2259	32 ± 10	Dib & Kaspi (2014)
CXOU J1714	2.1 ± 0.9	Sato et al. (2010)
	$2.2 \pm 0.9^*$	Halpern & Gotthelf (2010b)
	$1.7 \pm 0.5^*$	Halpern & Gotthelf (2010b)
Swift J1834	1.08 ± 0.04	Kargaltsev et al. (2012)

(Z.F. Gao et al. 2016, MNRAS, 5456, 55)

PSR J1640-4631 is the first pulsar reported with high braking index (n=3.15), it is also known as HESS J1640-465 and emits gamma-ray in TeV detectable using with NuSTAR and Chandra X-ray observatories, is associated with SNR G338.3-0.0.

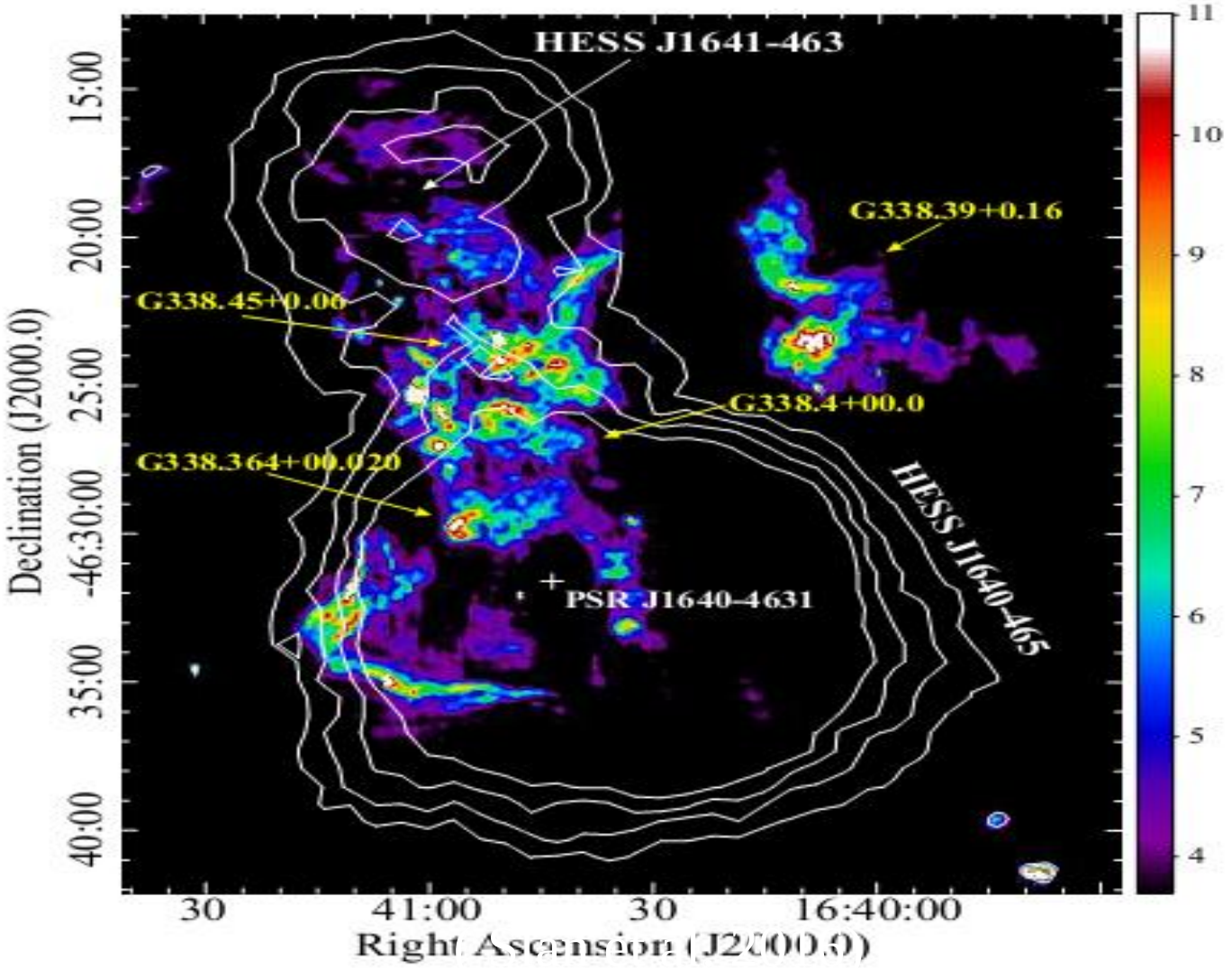

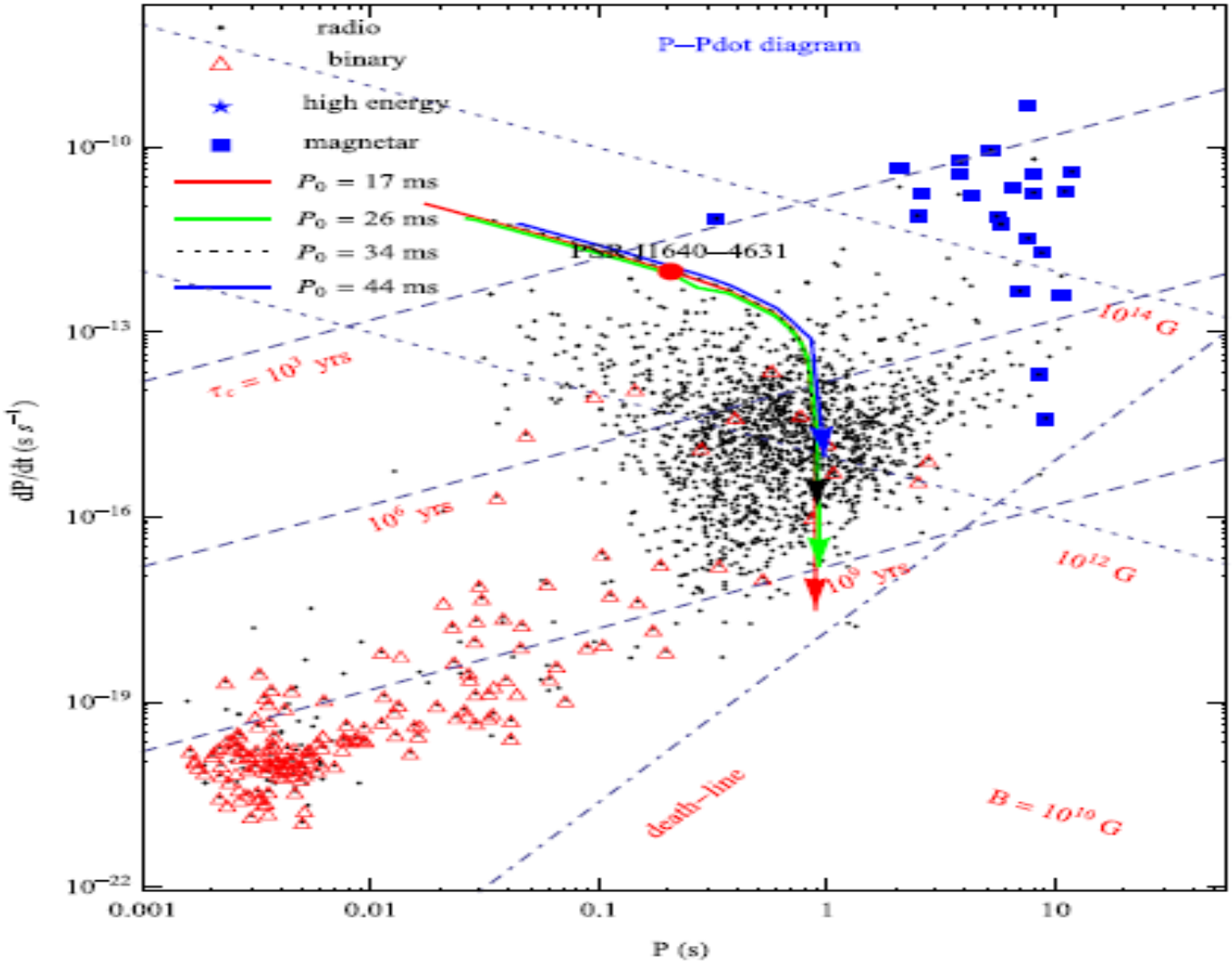

(Z.F. Gao et al. 2017, ApJ, 849, 19)

Improvements needed in our previous work

- In Gao et al. (2017), the assumption of a simple exponential decay of dipolar magnetic field during the first 10 kyr was made, but the combined ohmic decay and Hall drift may cause a qualitatively different form of field decay.

- The theoretical model in Gao et al. (2017) utilized the familiar flat space-time form of the Maxwell's equations The inclusion of relativistic effects raises the timescale of magnetic field ; it is necessary to re-investigate the dipole magnetic field of PSR J1640-4631 by considering the gravitational effects.

Sec. 2. The Ohmic decay of the dipole magnetic fields in PSR J1640-4631

2.1An eigenvalue equation for dipole magnetic field decay

- We assume spherically symmetric spacetime geometry and employ the familiar Schwarzschild coordinates, we can cast the spacetime geometry of a NS

$$ds^2 = -e^{2\Phi(r)}c^2t^2 + e^{2\lambda(r)}dr^2 + r^2d\Omega^2, \quad (2)$$

where $e^{\Phi(r)}$ is the red shift factor, $e^{\lambda(r)} = (1-2Gm(r)/c^2r)^{-1/2}$ is the space curvature factor and $m(r)$ is the gravitational mass enclosed within radius r.

- According to Wald (1984), Maxwell's equations in covariant forms is expressed as

$$\nabla^\alpha F_{\alpha\beta} = -\frac{4\pi}{c}J_\beta, \quad (3a)$$

$$\nabla_\alpha F_{\beta\gamma} = 0, \quad (3b)$$

where $F_{\alpha\beta} = -F_{\beta\alpha}$, and J_α are the coordinate components of the Maxwell tensor, the conserved four current respectively. The current is described by the relativistic extension of Ohm's law,

$$J_\alpha = \sigma g_{\alpha\beta}F^{\beta\gamma}V_\gamma, \quad (4)$$

where V^α and σ stand for the four velocity of a conducting neutral plasma

- To simplify the algebra, consideration is restricted to dipolar (poloidal) fields in this paper. In the curved spacetime, the MHD equation takes the following form:

$$\frac{1}{c}\frac{\partial \vec{B}_p}{\partial t} + \nabla \times \left[\frac{c}{4\pi\sigma}\nabla \times (e^{\Phi(r)}\vec{B}_p)\right] = 0, \qquad (5)$$

where $$\vec{B}_p = B^r \vec{r} + B^\theta \vec{\theta}, \qquad (6)$$

- The field components of (B^r, B^θ) are given by

$$B^r(t,r,\theta) = -F(t,r)\cos\theta, \qquad (7a) \qquad B^\theta(t,r,\theta) = \frac{1}{2r}\left(1 - \frac{2GM}{c^2 r}\right)^{\frac{1}{2}} \frac{\partial(r^2 F)}{\partial r}\sin\theta, \qquad (7b)$$

with the function *F(r,t)* to be determined.

- Assuming that magnetic field lines confined in the crust, we give

$$\frac{4\pi\sigma r^2}{c^2}\frac{\partial F}{\partial x^0} = (1 - \frac{2Gm(r)}{c^2 r})^{\frac{1}{2}}\frac{1}{r^2}\frac{\partial}{\partial r}\left[Z(1 - \frac{2Gm(r)}{c^2 r})^{\frac{1}{2}}\frac{\partial(r^2 F)}{\partial r}\right] - 2ZF \qquad (8)$$

with $Z \equiv (1 - 2M(R)/R)^{1/2}$.

Boundary conditions and relativistic Stokes function

- First, the field at the stellar surface must approach continuously to the field in vacuum, the outer boundary condition is given by

$$R\left.\frac{\partial(r^2F(t,r))}{\partial r}\right|_R = G(y)r^2F(t,R), \qquad (9a)$$ and $$G(y) = y\frac{2y\ln(1-y^{-1}) + \frac{2y-1}{y-1}}{y^2\ln(1-y^{-1}) + y + \frac{1}{2}} \qquad (9b)$$

with $y = R/R_S$, where $R_S \equiv 2GMR/c^2$ is Schwarzschild radius of the star, and M is the star's mass. Since $G(y)<0$ (in particular, in the flat spacetime case $G(\infty) = -1$), the boundary condition forces a bending of F in the upper layer.

- Secondly, $F(r,t)=0$ as $r \to 0$.
- By coupling Einstein's equations with a perfect fluid energy momentum tensor, we can obtain differential equations for $m(r)$, $\Phi(r)$ and the TOV equation of hydrostatic equilibrium $P(r)$.

$$\frac{4\pi\sigma}{c^2}e^{-\Phi(r)}\frac{\partial F}{\partial t} = (1-\frac{2Gm(r)}{c^2r})\frac{\partial^2F}{\partial r^2} + \frac{1}{r^2}\left[\frac{2Gm(r)}{c^2} + \frac{4\pi G}{c^2}r^3(\frac{P}{c^2}-\rho)\right]\frac{\partial F}{\partial r} - \frac{2F}{r^2} \qquad (10)$$

which needs to satisfy the relativistic Stokes function, we can expand $F(t,r)$ into a series

$$F(t,x) = \sum_n A_n e^{-\frac{c^2\lambda_n t}{4\pi\sigma R^2}}X_n(x) \ \ (n=1,2,3,\cdots), \qquad (11)$$

- where a variable defined as $x=r/R$, A_n is the expansion coefficient and the summation is over all eigenmodes, $X_n(x)$ of the corresponding Sturm-Liouville eigenvalue problem and the associated boundary-regularity conditions

$$Ł X_n(x) + \lambda_n e^{-\Phi} X_n(x) = 0, \qquad (12)$$

where $$Ł = (1 - \frac{2Gm(r)}{c^2 x})\frac{\partial^2}{\partial x^2} + \frac{1}{x^2}\left[\frac{2Gm(r)}{c^2} + \frac{4\pi G}{c^2}x^3(\frac{P}{c^2} - \rho)\right]\frac{\partial}{\partial x} - \frac{2}{x^2} \qquad (13)$$

is determined by the geometrical and hydrodynamical variables. By introducing the first-order spherical Bessel function $j_1(\xi) = (\sin\xi - \xi\cos\xi)/\xi^2$, we obtain

$$X_n(x) = \frac{1}{xR^2} j_1(n\pi x) = \frac{\sin(n\pi x) - n\pi x\cos(n\pi x)}{n^2\pi^2 R^3 x^2}. \qquad (14)$$

- Then the final expression of $F(t,x)$ is given by

$$F(t,x) = \sum_n A_n e^{\frac{-c^2\lambda_n t}{4\pi\sigma R^2}} X_n(x) = \sum_n A_n \frac{1}{xR^2} j_1(n\pi x) e^{\frac{-c^2\lambda_n t}{4\pi\sigma R^2}}, \qquad (15)$$

where $$A_n = \frac{\int_0^1 x j_1(n\pi x)x^2 dx}{\int_0^1 j_1^2(n\pi x)x^2 dx}, \qquad (16)$$

2.2An eigenvalue equation of toroidal magnetic field decay

- Similarly, the toroidal component of the field is given by

$$B_{\varphi} = -\sum_{lm} H_l(x,t)\frac{dY_{lm}}{d\theta} . \qquad (1)$$

- Here only the dipolar component is considered (taking l=1 and m=0). In order to facilitate the calculation, we prefer the force-free fields . They satisfy

$$\nabla \times \mathbf{B} = \mu \mathbf{B}, \quad \mathbf{B} \cdot \nabla \mu = 0, \qquad (2)$$

where μ is a parameter related to the magnetic field curvature, When magnetic fields are confined to the crust, μ must be adjusted to have a vanishing radial component in the crust-core interface, which can be done by solving

$$\tan[\mu(R_{\rm core} - R)] = \mu R_{\rm core} . \qquad (3)$$

- We find that H(r, t) has the same evolution form as that of F(r, t), which implies a simple linear relation

$$\frac{|B_{\varphi}|}{|B_r|} = \frac{H(r,t)}{F(r,t)} = \frac{\mu x R}{2} \qquad (4)$$

- Using separation of variables, we get

$$\frac{4\pi\sigma}{c}\frac{\partial H(r,t)}{\partial x^0} = (1-\frac{2M(r)}{r})^{\frac{1}{2}}\frac{1}{r^2}\frac{\partial}{\partial r}[Z(1-\frac{2M(r)}{r})^{\frac{1}{2}}\frac{\partial(r^2H(r,t))}{\partial r}] - \frac{2ZH(r,t)}{r^2}. \quad (5)$$

- Then, we have

$$H(t,x) = \frac{\mu x R}{2}\sum_n A_n \frac{j_1(n\pi x)}{xR^2} e^{\frac{-c^2\lambda_n t}{4\pi\sigma R^2}}. \quad (6)$$

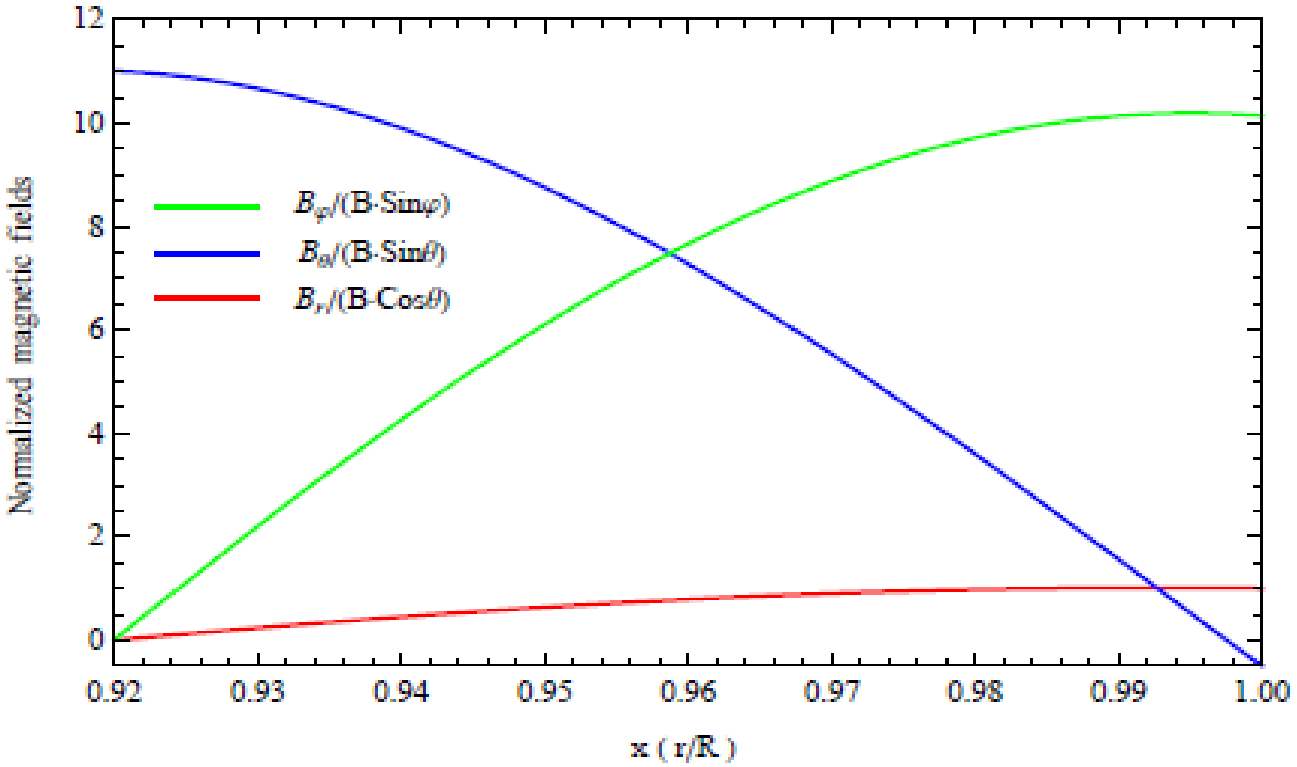

Normalized magnetic field components of the crustal confined for the force free field: vs. normalized radial coordinate x, $M = 1.45M_\odot, R = 1.16\times10^6\,\mathrm{cm}$ $R_{\mathrm{core}}/R \sim 0.92$.

EoS: Douchin \& Haensel (2001) $B_0 \sim 3.4\times10^{13}\,\mathrm{G}$ for PSR J1640-4631

Numerical fitting of the pure ohmic decay for PSR J1640-4631.

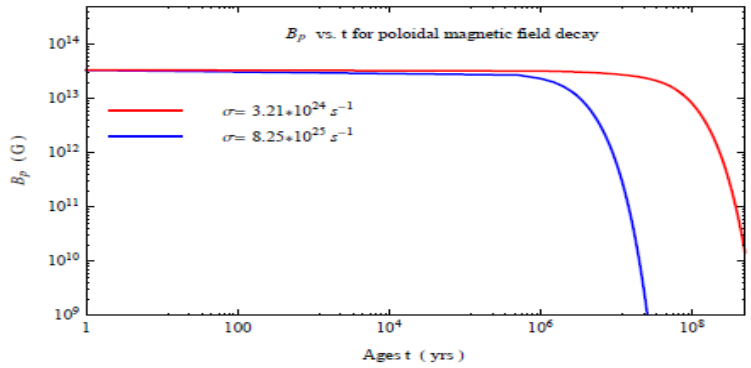

(a)

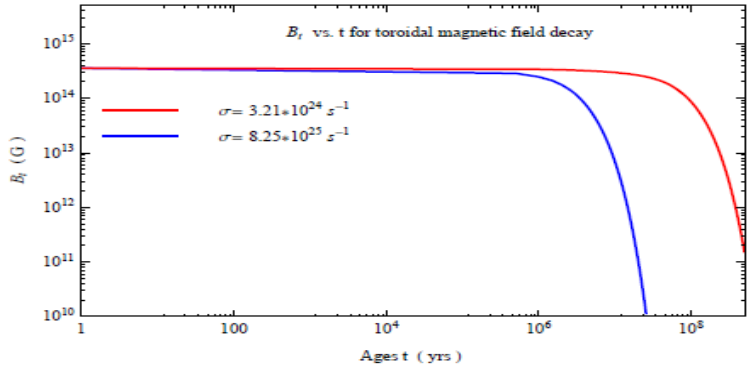

(b)

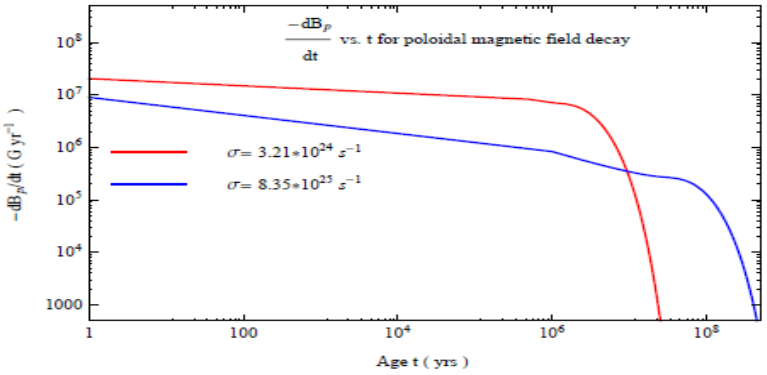

(c)

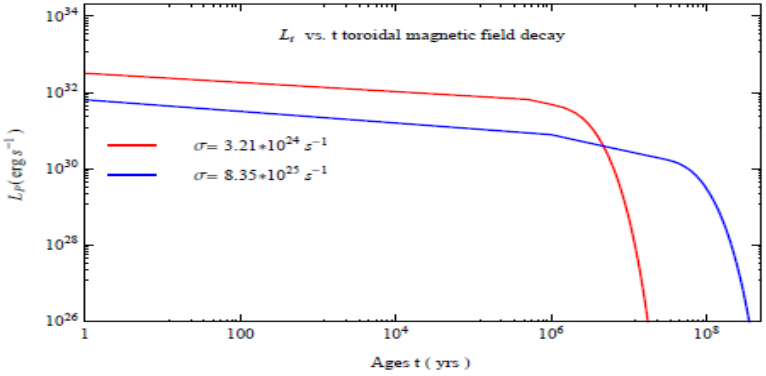

(d)

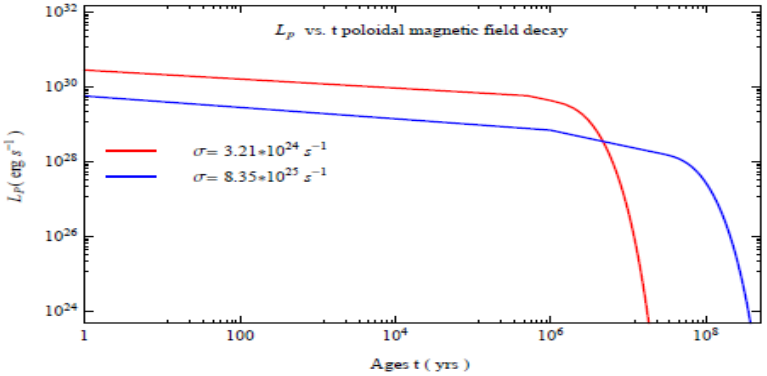

(e)

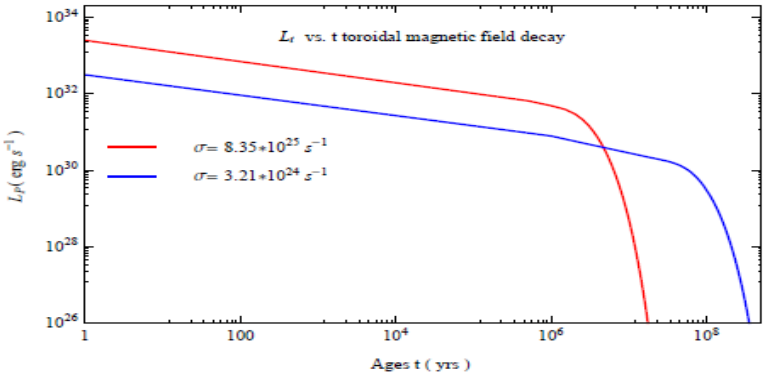

(f)

Sec.3 The coupled model of the ohmic decay and Hall drift

- In an enhanced ohmic decay model, the induction equation describing the evolution of poloidal magnetic fields in the crust is given by

$$\frac{\partial \mathbf{B}_p}{\partial t} = -\nabla\times\left[\frac{c^2}{4\pi\sigma}(e^{\Phi}\mathbf{B}_p) + \frac{c}{4\pi e n_e}[\nabla\times(e^{\Phi}\mathbf{B}_p)]\right]. \qquad (7)$$

- This equation contains two different effects: the Hall drift and ohmic decay, and each effect operates at different timescales:

$$\tau_{\rm Hall} = \frac{4\pi n_e e R_c^2}{cB_0} = \frac{1.6}{B_{14}}\left(\frac{R_c}{1{\rm km}}\right)^2 \frac{n_e}{2.5\times10^{36}\,{\rm cm}^{-3}}\,{\rm Myr},$$

$$\tau_{\rm Ohm} = \frac{4\pi\sigma R_c^2}{c^2} = 13.5\left(\frac{R_c}{1{\rm km}}\right)^2 \frac{\sigma}{3.0\times10^{24}\,{\rm s}^{-1}}\,{\rm Myr}. \qquad (8)$$

- We include phenomenologically two evolutionary stages: an initial stage with rapid (non-exponential) decay, and a later stage with purely ohmic dissipation

$$B_p = B_0\frac{exp(-Zt/\tau_{\rm Ohm})}{1+\frac{\tau_{\rm Ohm}}{\tau_{\rm Hall}}(1-exp(-Zt/\tau_{\rm Ohm}))}. \qquad (9)$$

- The poloidal magnetic energy decay rate, L_p , in the crust in the enhanced ohmic decay model is then estimated as

$$L_p = \frac{1}{4\pi}\int_V \left(\frac{B_p^2}{\tau_{\rm Ohm}} + \frac{B_p^3}{\tau_{\rm Hall} B_0}\right) dV \qquad (10)$$

$$= \int B_0^2 \left(\frac{exp(-2Zt/\tau_{\rm Ohm})}{\tau_{\rm Ohm}[1+\frac{\tau_{\rm Ohm}}{\tau_{\rm Hall}}(1-exp(\frac{-Zt}{\tau_{\rm Ohm}}))]^2} + \frac{exp(-3Zt/\tau_{\rm Ohm})}{\tau_{\rm Hall}[1+\frac{\tau_{\rm Ohm}}{\tau_{\rm Hall}}(1-exp(\frac{-Zt}{\tau_{\rm Ohm}}))]^3}\right) r^2 dr.$$

- Using Eq. (10), we calculate the current values of L_p as $1.25 \times 10^{30}\,{\rm erg\,s^{-1}}$ and $1.77 \times 10^{30}\,{\rm erg\,s^{-1}}$ respectively, corresponding to $\tau_{\rm Ohm} = 3.25 \times 10^8\,{\rm yrs}$ and $\tau_{\rm Ohm} = 1.26 \times 10^7\,{\rm yrs}$, , respectively.

- From the x-ray observations for PSR J1640-4631

$$F_{PSR} = 1.9\times10^{-13}\ {\rm erg\ cm^{-2}\ s^{-1}}$$

$$d = 12{\rm kpc} = 12\times3.08\times10^{19}\ {\rm m}$$

For magnetars

$$T_S \sim (4-10)\times10^6\ {\rm K}$$

$$L_X = F_{PSR}\times 4\pi d^2 = 3.26\times10^{33}\ {\rm erg\,s^{-1}}$$

$$T_s = (L_s/4\pi R^2\sigma_{SB})^{1/4} = (L_X/4\pi R^2\sigma_{SB})^{1/4} \approx 1.25\times10^6\ {\rm K}$$

Numerical fitting for the enhanced ohmic decay in PSR J1640-4631

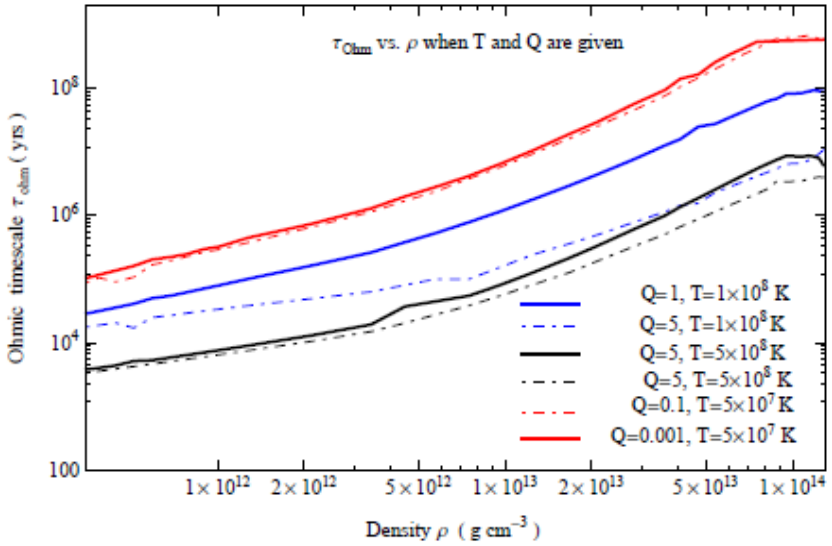

(a)

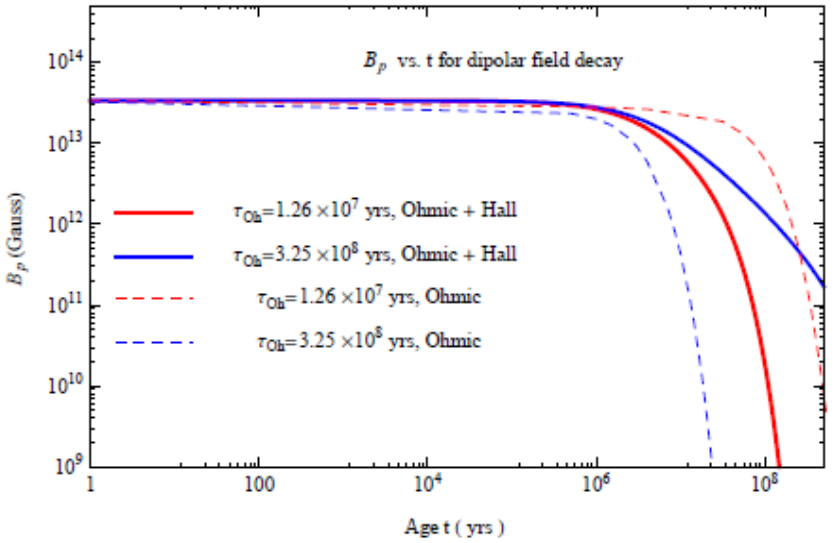

(b)

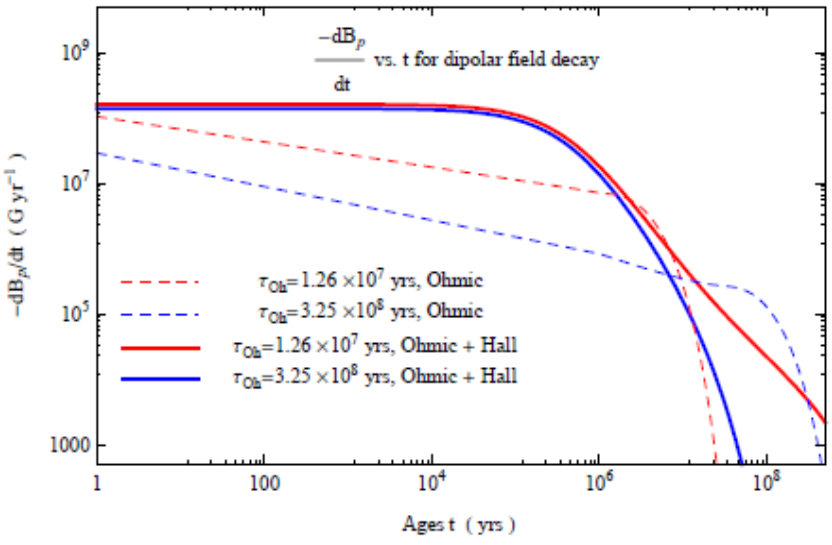

(c)

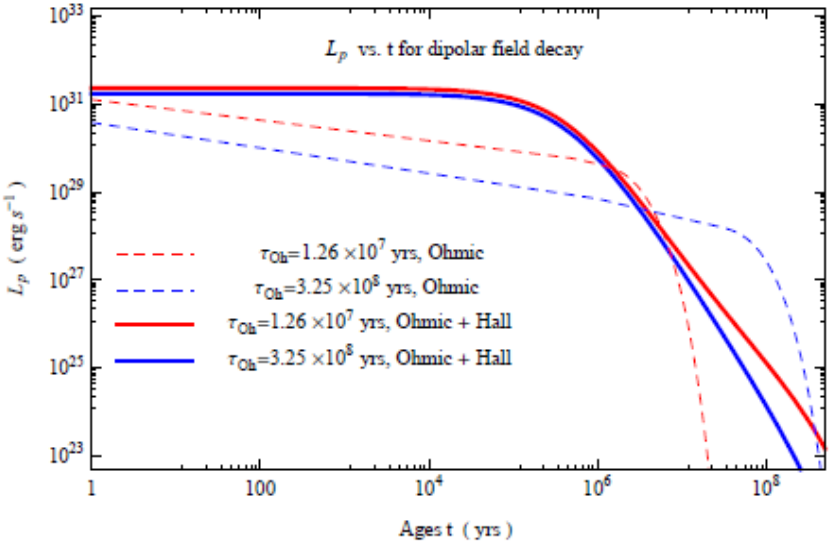

(d)

Other isotropic internal heating mechanisms

- The minimal cooling model (Page et al. 2004, 2006);
- Superfluid vortex creeping) (Alpar et al. 1984, 1989; Cheng et al. 1992)
- The rotochemical heating (Gonzalez \& Reisenegger 2010)

Sec.4 Anisotropic heating for soft X-ray emission

4.1Magnetic spot formation in NSs

- The partially screened gap (PSG) model implies an additional constraint on the local intensity of small-scale magnetic field strength. The magnetic spots can be created by extracting magnetic energy from the toroidal field that resides in deep crustal layers, via the Hall drift with a timescale of 10 kyrs (Geppert \& Vigano 2014). The formation of magnetic spots in the crust would have consequences for the potentially observable surface temperature distribution.

- The magnetic induction equation and the thermal balance equation show a tight connection of thermal and magnetic evolution

$$\frac{\partial \mathbf{B}}{\partial t} = -\nabla \times \left[\frac{c^2}{4\pi\sigma}(e^{\Phi}\mathbf{B}) + \frac{c}{4\pi e n_e}[\nabla \times (e^{\Phi}\mathbf{B})] \right],$$

$$c_v \frac{\partial T}{\partial t} - \nabla \cdot [e^{\Phi}\hat{\kappa} \cdot \nabla (e^{\Phi} T] = e^{2\Phi}(-Q_\nu + Q_h),$$

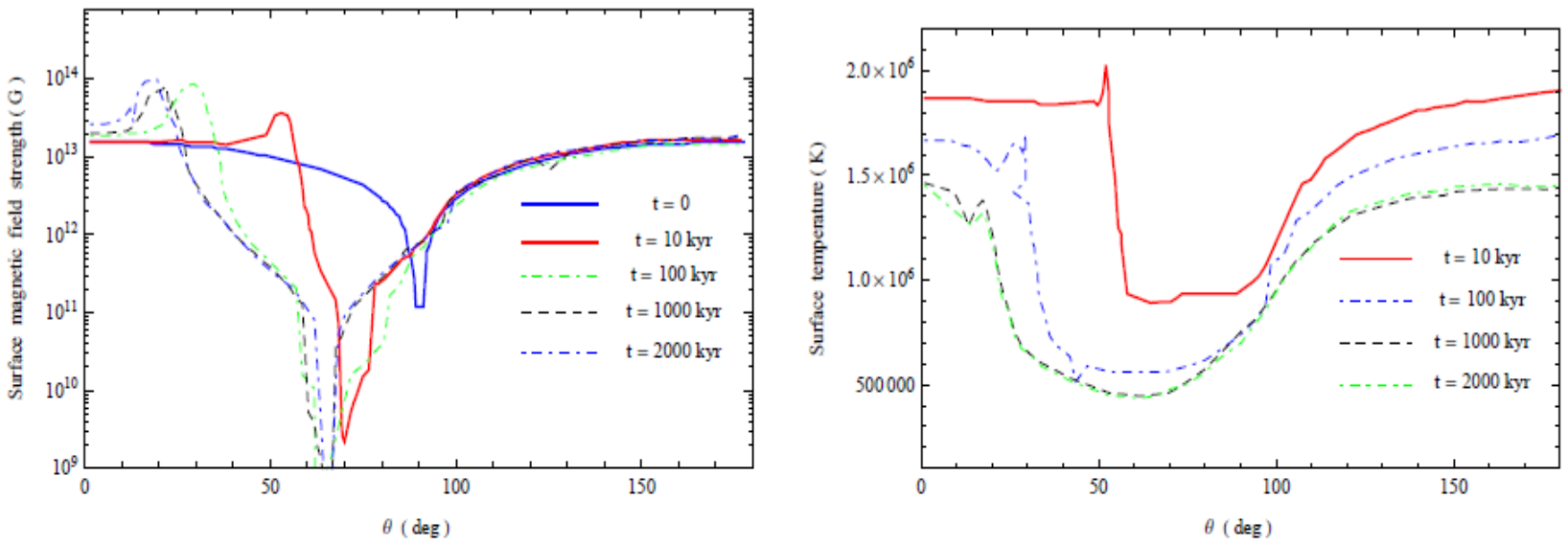

Fig. 4.— (a) Evolution of magnetic field of PSR J1640−4631 at $t = 0$ (blue solid line), 10 kyr (red solid line), 100 kyr (green dash-dotted), 1000 kyr (black dashes) and 2000 kyr (blue dash-dotted). (b) Evolution of the surface redshifed temperature PSR J1640−4631 at $t = 10$ kyr (red solid line), 100 kyr (blue dash-dotted), 1000 kyr (black dashes) and 2000 kyr (green dash-dotted).

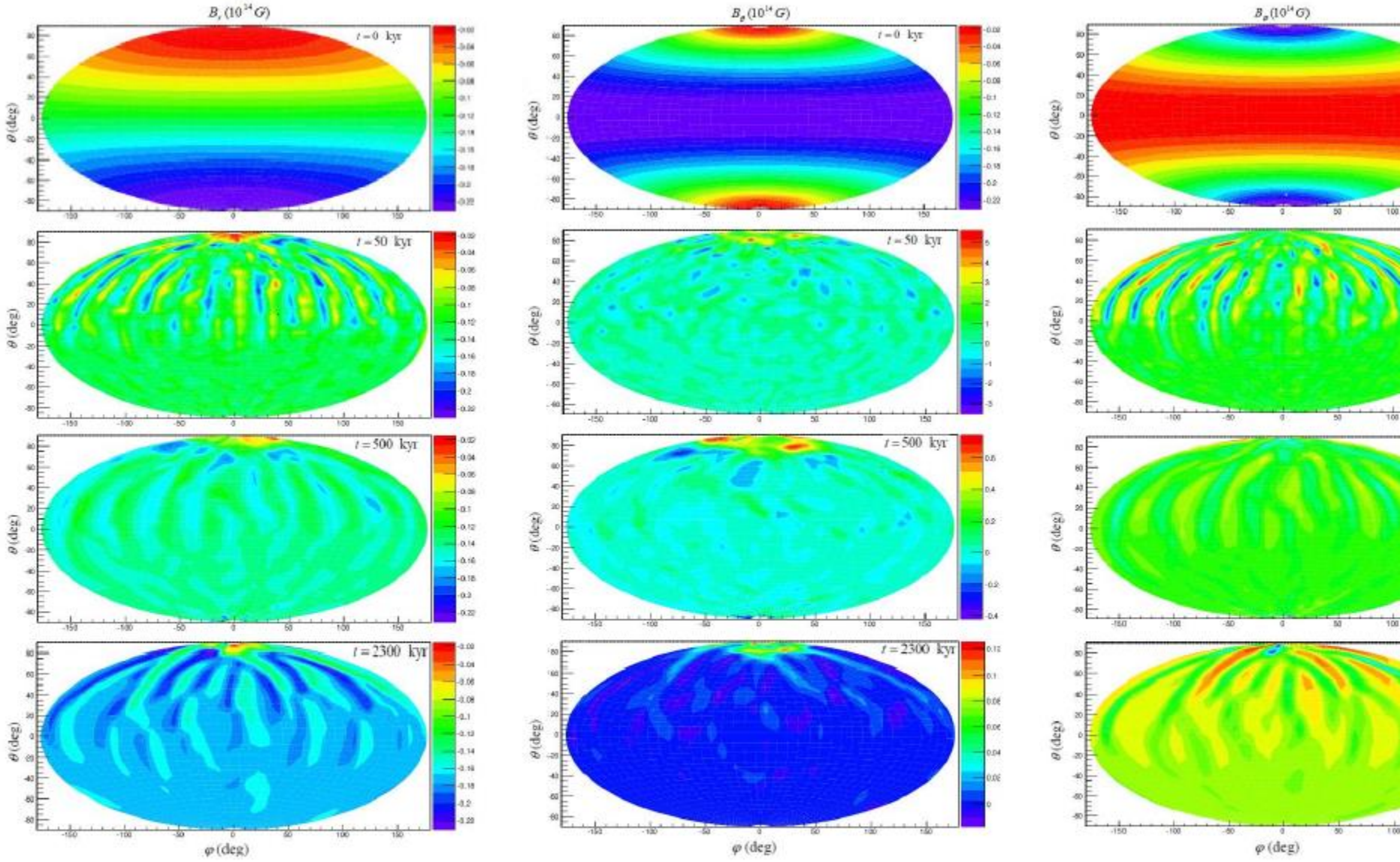

Fig. 5.— Contour plots of three components of magnetic fields in PSR J1640−4631. The plots are made Hammer projection at a $r = 0.995R$ for run A99-4, where 99% of the initial energy is in the toroidal field.

4.2Thermoplastic wave heating due to toroidal field decay

- The rapid development of stability in the crust of a highly magnetized NS yields stress (Beloborodov \& Li 2016). A plausible mechanism for yielding this instability is a thermoplastic flow, which occurs in hot crust with T >10^8 K (e.g., Yuan \& Zhang 1998, 1999). This possibility is attractive for the inner crust under the polar caps of the star (Beloborodov \& Levin 2014).
- In a magnetically stressed crust, thermal softening leads to a TPW that is the temperature sensitive plastic flow. Heat conduction helps the burning to spread, and the propagation wave dissipates the magnetic energy inside the crust.

$$B_\phi \sim 6.3\times10^{12} n_{e,33}^{4/3}\left(\frac{2000\,\mathrm{yr}}{\tau_{\mathrm{Hall}}}\right)\mathrm{G},$$

$$\dot{q}\sim\frac{B_\phi^2}{8\pi\triangle t}\sim\frac{B_\phi^2 v^2}{8\pi\chi}\geq\frac{B_\phi^2}{8\pi\chi}\left(\frac{\dot{\psi}_{\mathrm{ohm}} r_0}{2b_0}\right)^2,$$

$$L_X=\dot{q}V_p=S_p\sigma T_p^4,$$

$$F_X^\infty=\left(\frac{R}{d_{12}}\right)^2 F_X(1-r_g/R)^2,$$

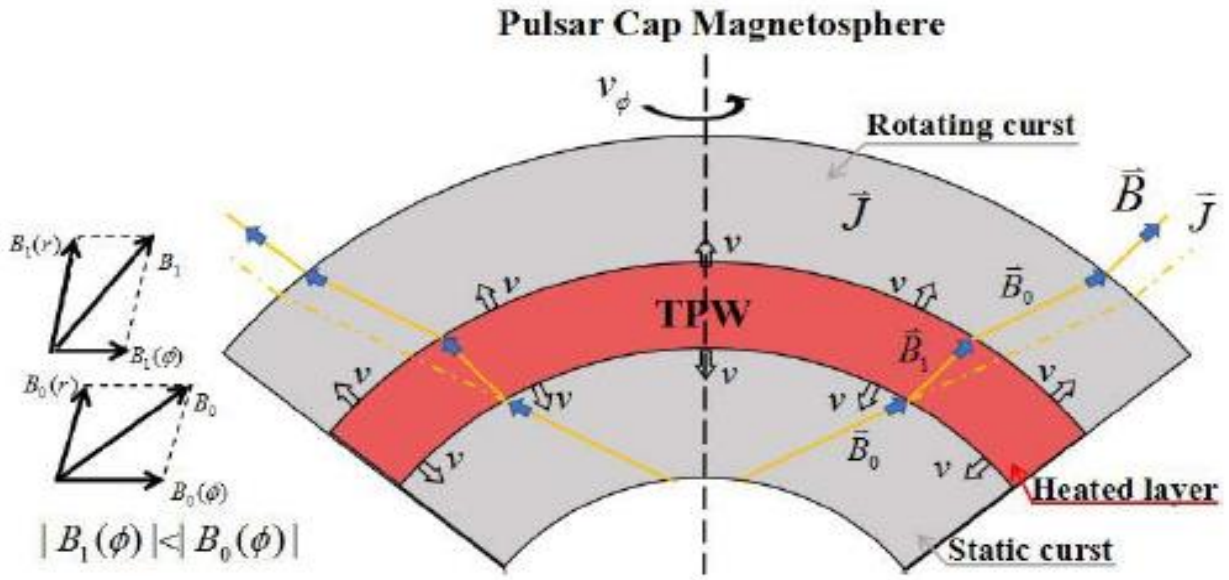

Fig. 6.— Crustal plate, that locates above the plastically heated layer, rotates very slowing with horizontal velocity v_ϕ.

Efficiency of soft X-ray emission

The surface temperature T_* at the non-polar cap region is less than that in the polar cap. We estimate T_* as

$$T_* = T_{\rm p}(\frac{2cP}{\pi R})^{-1/4} = (2.02 - 2.65) \times 10^5\,{\rm K} \quad (61)$$

for a possible density range $\rho \sim (6-9) \times 10^{13}\,{\rm g\,cm^{-3}}$. The X-ray emission from the non-polar cap region may be powered by the combined effects from the ohmic decay of magnetic field, superfluid vortex creeping, rotochemical heating and so on. Due to the lower temperature, the X-ray flux at the non-polar cap region may be below the minimum limit of the X-ray detector. In theory, the resulting X-ray luminosity can be estimated as

$$L_X^{'} = (4\pi R^2 - S_p)\sigma T_*^4. \quad (62)$$

Then the total soft X-ray luminosity of the star is

$$L_{tot}(X) = L_X^{'} + L_X\,, \quad (63)$$

and the X-ray energy conversion coefficient is given by

$$\eta = \frac{L_{tot}(X)}{L_{rot} + L_B + Q} \approx (1.4 \sim 4.7) \times 10^{-6}. \quad (64)$$

This value of η is less than the isotropic X-ray energy

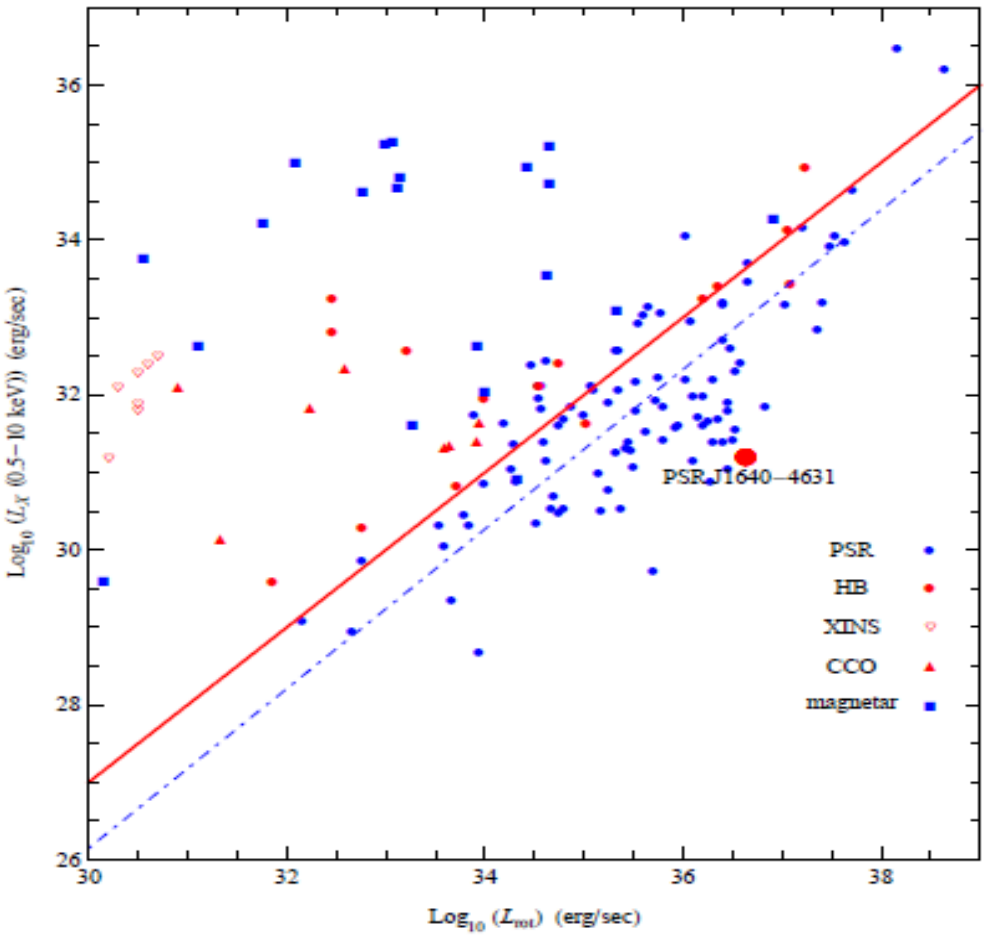

Fig. 7.— The $L_X - L_{rot}$ plot for our sample and related objects. The big filled red-dot indicates PSR J1640−4631.

Summary

In this work, we investigate the Ohmic decay of surface dipole magnetic field of high-braking index pulsar PSR J1640−4631, and interpret the observed soft X-ray flux $F_x^{\infty}[2-10\mathrm{keV}]$ from $Chandra + NuStar$ telescopes. We obtain the ohmic decay timescale $\tau_{\mathrm{ohm}} \sim 3.23 \times 10^6$ yr. Observations indicate that magnetic multipole fields could exist in a neutron star and the toroidal component of multipole fields at and near the pulsar cap is thought to be responsible for the star's unique pulse profile. A possible application of ohmic decay timescale to thermoplastic wave (TPW) heating due to toroidal fields dispassion is studied for interpreting the observed soft x-ray emission of PSR J1640−4631, and other heating mechanisms for the star's surface thermal emission are also investigated.

Thank you

for your attention!